Clim Dyn
DOI 10.1007/s00382-012-1385-1

A study of impact of the geographic dependence of observing system on parameter estimation with an intermediate coupled model

Xinrong Wu · Shaoqing Zhang · Zhengyu Liu · Anthony Rosati · Thomas L. Delworth

Received: 18 January 2012 / Accepted: 26 April 2012

Abstract Observational information has a strong geographic dependence that may directly influence the quality of parameter estimation in a coupled climate system. Using an intermediate atmosphere-ocean-land coupled model, the impact of geographic dependent observing system on parameter estimation is explored within a "twin" experiment framework. The "observations" produced by a "truth" model are assimilated into an assimilation model in which the most sensitive model parameter has a different geographic structure from the "truth", for retrieving the "truth" geographic structure of the parameter. To examine the influence of data-sparse areas on parameter estimation, the twin experiment is also performed with an observing system in which the observations in some area are removed. Results show that traditional single-valued parameter estimation (SPE) attains a global mean of the "truth", while geographic dependent parameter optimization (GPO) can retrieve the "truth" structure of the parameter and therefore significantly improves estimated states and model predictability. This is especially true when an observing system with data-void areas is applied, where the error of state estimate is reduced by 31 % and the corresponding forecast skill is doubled by GPO compared with SPE.

Keywords Observing system · Geographic dependence · Parameter estimation · Coupled model

Abbreviations

EAKF	Ensemble adjustment Kalman filter
SPE	Single value parameter estimation
GPO	Geographic dependent parameter optimization
SEO	State estimation only
CTL	Model free control run
SST	Sea surface temperature
LST	Land surface temperature

1 Introduction

Parameter estimation in a coupled climate model has received increasing attention due to its potential in the reduction of model bias and the improvement of climate predictability. In data assimilation theory (e.g. Jazwinski 1970), parameter estimation can be realized by including model parameters into assimilation control variables (e.g. Banks 1992a, b; Anderson 2001; Hansen and Penland 2007; Zhang et al. 2011; Kang 2009; Kang et al. 2011). So far, parameter estimation has been implemented mostly in an idealized experimental framework and model observing system (e.g. Annan and Hargreaves 2004; Aksoy et al. 2006a, b; Kondrashov et al. 2008; Tong and Xue 2008a, b;

X. Wu (✉)
GFDL-Wisconsin Joint Visiting Program, Princeton, NJ, USA
e-mail: xinrong.wu@noaa.gov

X. Wu
Key Laboratory of Marine Environmental Information Technology, State Oceanic Administration, National Marine Data and Information Service, Tianjin, People's Republic of China

S. Zhang · A. Rosati · T. L. Delworth
GFDL/NOAA, Princeton University, Princeton, NJ, USA

Z. Liu
Department of Atmospheric and Oceanic Sciences, Center for Climate Research, University of Wisconsin-Madison, Madison, WI, USA

Z. Liu
Laboratory of Ocean-Atmospheric Studies, Peking University, Beijing, People's Republic of China

Published online: 17 May 2012

Zhang 2011a, b) for exploration. In the real world, however, a coupled general circulation model (CGCM) is used to assimilate instrumental data for climate estimation and prediction initialization. The observation-based parameter estimation depends on the model sensitivity and the observing system, both of which are geographic dependent. Recently, Wu et al. (2012) investigated the impact of the geographic dependence of model sensitivity on parameter estimation with an intermediate coupled model, and presented a new parameter estimation scheme, called geographic dependent parameter optimization (GPO). As a follow-up study, here we use the same model to examine the impact of geographic dependent observing system on parameter estimation. The observational information has two types of geographic dependence. First, the data coverage of the observing system has geographic dependence. Second, physical processes in the climate system are geographically dependent (mixing in the ocean and convection in the atmosphere for instance) which leads that the representation of observations is geographic dependent.

A twin experiment framework is designed to carry out this study. First, to simulate the geographic dependence of the representation of observed values, we set a sensitive parameter in the model to have geographic structures. Second, to study the impact of the geographic dependence of data coverage of an observing system, the twin experiment is also performed when observations in certain areas are removed. Based on such twin experimental settings, we compare three sets of experiment results throughout this study: (1) state estimation only (SEO) that only assimilates observations into model states; (2) single-valued parameter estimation (SPE) that performs both state and parameter estimations but not allowing parameter to vary geographically and (3) geographic dependent parameter optimization (GPO) that optimizes model parameters according to local observational information and model sensitivity thus allowing the parameter to vary geographically.

This paper is organized as following: after the methodology section that briefly describes the model and the GPO scheme as well as the twin experimental setting, Sect. 3 presents the impact of geographic dependence of observing system on parameter estimation. Section 4 examines the impact of different parameter estimation schemes on model predictability. Summary and general discussions are given in Sect. 5.

2 Methodology

2.1 An intermediate coupled model

To clearly illustrate the impact of the geographic dependence of observing systems on parameter estimation and avoid the complexity of a CGCM, an intermediate atmosphere–ocean-land coupled model (Wu et al. 2012) is employed. Here, we briefly review the coupling scheme of this model.

The atmosphere is a global barotropic spectral model based on the equation of potential vorticity conservation:

$$\frac{\partial q}{\partial t} + J(\psi, q) = \begin{cases} \lambda(T_o - \mu\psi) & \text{ocean} \\ \lambda(T_l - \mu\psi) & \text{land} \end{cases} \tag{1}$$

where $q = \beta y + \nabla^2\psi$, $\beta = \mathrm{d}f/\mathrm{d}y$, f denotes Coriolis parameter, y represents the northward meridional distance from the equator, ψ represents the geostrophic atmosphere streamfunction. T_o and T_l denote sea surface temperature (SST) and land surface temperature (LST) respectively.

The ocean consists of a 1.5-layer baroclinic ocean with a slab mixed layer (Liu 1993) and the simulated upwelling by a streamfunction equation as

$$\begin{cases} \dfrac{\partial}{\partial t}\left(-\dfrac{\varphi}{L_0^2}\right) + \beta\dfrac{\partial}{\partial x}\varphi = \gamma\nabla^2\psi - K_q\nabla^2\varphi \\ \dfrac{\partial}{\partial t}T_o + u\dfrac{\partial T_o}{\partial x} + v\dfrac{\partial T_o}{\partial y} - K_h\varphi = -K_T T_o + A_T\nabla^2 T_o \\ +s(\tau, t) + C_o(T_o - \mu\psi) \end{cases} \tag{2}$$

where φ is the oceanic streamfunction; $L_0^2 = g'h_0/f^2$ is the oceanic deformation radius; $K_h = K_T \times \kappa \times f/g'$ (Philander et al. 1984) represents the strength of upwelling (downwelling); $s(\tau, t) = K_T \times s_0(\tau) \times [1-(\tau/4{,}500 + 1/200) \times \cos(2\pi(t-15)/360)]$ is the solar forcing, where s_0 represents the annual-mean solar forcing with zonal distribution, τ denotes latitude, t is the current time steps in days. The period of solar forcing is set to 360 days, which defines the model calendar year.

The evolution of LST is simulated simply by a local linear equation

$$m\frac{\partial}{\partial t}T_l = -K_L T_l + A_L\nabla^2 T_l + s(\tau, t) + C_l(T_l - \mu\psi) \tag{3}$$

The coupled model is forwarded by a leap frog time stepping with a half hour integration step-size. An Asselin-Robert time filter (Robert 1969; Asselin 1972) is introduced to damp spurious computational modes in the leap frog time integration. Default values and meanings of all parameters are listed in Table 1. Last fourteen parameters are empirically determined by trial-and-error tuning. Note that the solar forcing $s(\tau, t)$ will not change once it is determined using the default value of K_T, so it acts as a part of the "dynamic core."

2.2 Brief review of a geographic dependent parameter optimization (GPO) scheme

GPO (Wu et al. 2012) is an extension of a coupled data assimilation scheme with enhanced parameter correction (DAEPC, Zhang et al. 2011). The ensemble adjustment

Table 1 Default values and meanings of parameters

Parameter	Meaning	Value	Nature of the value
r	Radius of earth	6.365×10^6 m	Untunable constant
Ω	Angular velocity of the earth	7.292×10^{-5} rad/s	‘’
g'	Reduced gravity	0.026 ms^{-2}	‘’
λ	Flux coefficient of the atmosphere	223 s^{-2} K^{-1}	Empirically tuning
μ	Dimensional conversion factor	2.2×10^{-7} m^{-2} sK	‘’
h_0	Mean thermocline depth	500 m	‘’
γ	Momentum coupling coefficient	10^{-5}/(100 days)	‘’
K_q	Diffusive coefficient of oceanic streamfunction	10^{-5}	‘’
κ	Ratio between upwelling and damping	1/6 Km^{-1}	‘’
K_T	Damping coefficient of sea surface temperature	1/(180 days)	‘’
A_T	Diffusive coefficient of sea surface temperature	10^4 m^2 s^{-1}	‘’
C_o	Flux coefficient of the ocean	10^{-8} Km^{-2}	‘’
m	Ratio of heat capacity between the land and the ocean	0.1	‘’
K_L	Damping coefficient of land surface temperature	1/(180 days)	‘’
A_L	Diffusive coefficient of land surface temperature	10^4 m^2 s^{-1}	‘’
C_l	Flux coefficient of the land	10^{-8} Km^{-2}	‘’
η	Asselin-Robert filter coefficient	0.01	‘’

Kalman filter (EAKF, Anderson 2001) is used to perform the simultaneously state estimation and parameter estimation in this study. EAKF is a sequential implementation of Kalman filter (Kalman 1960; Kalman and Bucy 1961) under an “adjustment” idea. While the sequential implementation provides much computational convenience for data assimilation, the EAKF maintains the nonlinearity of background flows as much as possible (Anderson 2001, 2003). Based on the two-step EAKF (Zhang and Anderson 2003), parameter estimation is a process similar to multivariate adjustment in state estimation. The first step computes the observational increment (Zhang et al. 2007) using

$$\Delta y_{k,i} = \left(\bar{y}_k^u + \Delta y'_{k,i}\right) - y_{k,i}^p \tag{4}$$

where $\Delta y_{k,i}$ represents the observational increment of the kth observation, y_k, for the ith ensemble member; $\bar{y}_k^u$ is the posterior mean of the kth observation; $\Delta y'_{k,i}$is the updated ensemble spread of the kth observation for the ith ensemble member; $y_{k,i}^p$ is the ith prior ensemble member of the kth observation. The second step that projects the observational increment onto relevant parameters can be formulated as

$$\Delta\beta_{k,i} = \frac{\mathrm{cov}(\beta, \mathrm{y_k})}{\sigma_k^2}\Delta y_{k,i}. \tag{5}$$

Here $\Delta\beta_{k,i}$ indicates the contribution of the kth observation to the parameter β for the ith ensemble member. cov(β, y_k) denotes the error covariance between the prior ensemble of parameter and the model-estimated ensemble of y_k. σ_k is the standard deviation of the model-estimated ensemble of y_k.

DAEPC is a modification of the standard data assimilation with adaptive parameter estimation (e.g. Kulhavy 1993; Borkar and Mundra 1999; Tao 2003). Since the successfulness of parameter estimation entirely depends on the accuracy of the state-parameter covariance (Zhang et al. 2011), and that model parameters do not have any dynamically-supported internal variability, the accuracy of the ensemble-evaluated covariance is determined by the accuracy of the model ensemble simulating the intrinsic uncertainty of the states for which the observations try to sample. After state estimation reaches “quasi-equilibrium” (QE), parameter uncertainty contributes much to the error of model state so that signal dominates the parameter-observation covariance. A norm of model state adjustments is used to determine whether state estimation has reached a QE state. Then parameters are adjusted using Eq. (5). The updated parameters are applied to the next data assimilation cycle, which further refines the state estimates.

The inflation scheme of DAEPC based on model sensitivities of parameters (Zhang et al. 2011; Zhang 2011a, b) is a particular aspect of DAEPC which is formulated as

$$\tilde{\boldsymbol{\beta}}_l = \bar{\beta}_l + \max\left(1, \frac{\alpha_0\sigma_{l,0}}{\sigma_l\sigma_{l,t}}\right)\left(\boldsymbol{\beta}_l - \bar{\beta}_l\right). \tag{6}$$

where $\boldsymbol{\beta}_l$ and $\tilde{\boldsymbol{\beta}}_l$ represent the prior and the inflated ensemble of the parameter β_l, $\sigma_{l,t}$ and $\sigma_{l,0}$ denote the prior spreads of β_l at time t and the initial time, α_0 is a constant

tuned by a trial-and-error procedure. σ_l is the sensitivity of the model state with regard to β_l. The over bar represents the ensemble mean.

Based on DAEPC, GPO localizes both the parameter and its sensitivity, then signals in parameter estimation can be significantly enhanced and the optimal parameter can be obtained under local least square frame (Wu et al. 2012).

2.3 Twin experiment design

A "twin" experiment is designed to explore the impact of the geographic dependence of observing system on parameter estimation. In order to simulate the geographic dependence of the observational representation, we set the most sensitive parameter (Wu et al. 2012), K_T, in the "truth" model is latitude-dependent. For 90°S and 90°N, K_T is set to the default value, while linearly reducing to 95 % of the default value at equator. Other 13 empirical parameters keep their default values without spatial variation. Then with this parameter configuration, starting from initial conditions $\mathbf{Z}_0 = (\psi^0, \varphi^0, T_o^0, T_l^0)$, where $\varphi^0 = 0$, ψ^0, T_o^0 and T_l^0 are zonal mean values of corresponding climatological fields, the coupled model is run for 101 years to generate time series of the "truth" with the first 50-year being the spin-up period. "Observations" of model states are generated by adding a Gaussian white noise that simulates observational errors to the relevant "true" states of the rest 51 years at specific observational frequencies. The standard deviations of observation relative to the truth are 10^6 m^2 s^{-1} for ψ, 100 m^2 s^{-1} for φ, 1 K for T_o and T_l respectively, while corresponding sampling frequencies are 6 h (for ψ), 1 day (for φ, T_o and T_l). In this study, the "observation" locations of ψ are global randomly and uniformly distributed with the same density of the model grids, while the "observation" locations of φ, T_o and T_l are simply placed at 5° × 5° global grid points which start from (0°E, 85°S) at the left-lower corner to (355°E, 85°N) at the right-upper corner. In order to simply simulate the geographic dependence of observational coverage, observations of T_o within mid-latitude North Pacific (180°E–205°E; 20°N–45°N) are removed. The ensemble size is set to 20 throughout this study, because a larger number did not change significantly the results.

To roughly simulate the real world scenario in which both the assimilation model and the assimilation initial condition are biased relative to observations, in our assimilation model, K_T is set to 10 % greater than the global mean of the "truth" values while other 13 parameters keep their default values. Starting from $\mathbf{Z}_0$, the biased model is spun-up for 50-year to generate the biased initial model states $\mathbf{Z}_1 = (\psi^1, \varphi^1, T_o^1, T_l^1)$. Then, the ensemble initial conditions of ψ are produced by superimposing a Gaussian white noise with the standard deviation of 10^6 m^2 s^{-1} on ψ^1, while φ, T_o and T_l are unperturbed. In addition, initial standard deviation of K_T is set to 1 % of the biased value, while other parameters are not perturbed. We denote the ensemble initial conditions of the coupled model as $\mathbf{\Pi}$.

Table 2 Observation-adjusted model variables and observation-optimized model parameter in the assimilation

	ψ^o	φ^o	T_o^o	T_l^o
State estimation	ψ	φ	T_o	T_l
Parameter optimization	–	–	T_o, K_T	–

Starting from $\mathbf{\Pi}$, an ensemble control run is integrated for 51 years without observational constraint (denoted as CTL) and the SEO is also performed. Then, parameter estimation experiments are started at the end of the first year where the state estimation has reached its quasi-equilibrium. Leaving out another 3 years as the spin-up period for parameter estimation, the evaluations of all assimilation schemes are based on the results of the last 47 years. Table 2 lists observation-adjusted model variables and observation-optimized model parameter in the assimilation. Here, ψ^o, φ^o, T_o^o and T_l^o represent observations; ψ, φ, T_o and T_l denote model states to be estimated; K_T is the parameter to be estimated. A two-time level adjustment (Zhang et al. 2004) is employed for state estimation. Additionally, in order to remove spurious correlations caused by long distance, a distance factor (Hamill et al. 2001) is introduced into the filtering. For ψ and T_l, the impact radius of observations is set to 500 km; while for φ and T_o, it is set to 1,000 km × cos(min(τ, 60)), where τ denotes the latitude of model grid.

3 Impact of the geographic dependence of observing system on parameter estimation

In this section, impacts of the geographic dependence of T_o observing system on traditional single-value parameter estimation (SPE) and GPO are investigated. Before parameter optimization starts, we compute the norm of model state adjustments to ensure that the state estimation reaches quasi-equilibrium (Zhang et al. 2011), roughly determining the state estimation spin-up period as 1 year.

For the inflation scheme of parameter ensemble, the ensemble spread of a model prognostic variable when a perturbation is added on a parameter is used to evaluate the relevant sensitivities quantitatively. For SPE, σ_l in Eq. (6) simply takes the time–space mean of the sensitivities of SST to K_T. α_0 is set to σ_l after trial-and-error tuning. At each analysis step, SPE uses all available observations of T_o to adjust the ensemble of K_T sequentially.

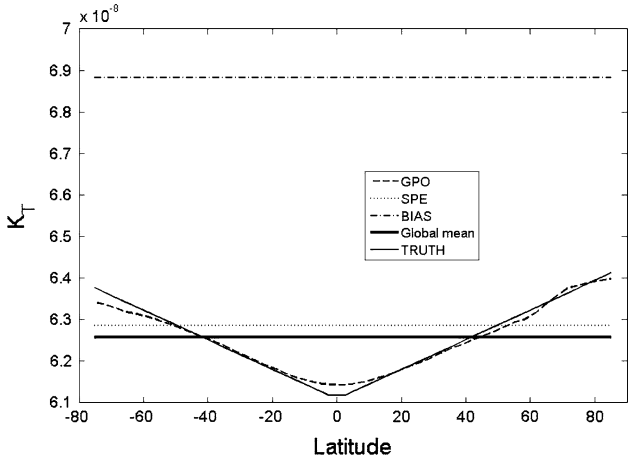

Fig. 1 Meridional distributions of the damping coefficient (K_T) of SST, where the *dashed line* represents the time-zonal averaged geographic dependent parameter optimization (GPO) optimized K_T; the *dotted line* indicates the time-averaged single-value parameter estimation (SPE) estimated K_T; the *dotted-dashed line* is the initial biased K_T; the *thick solid line* shows the global mean of the "truth" values; the *thin solid line* is the "truth" value

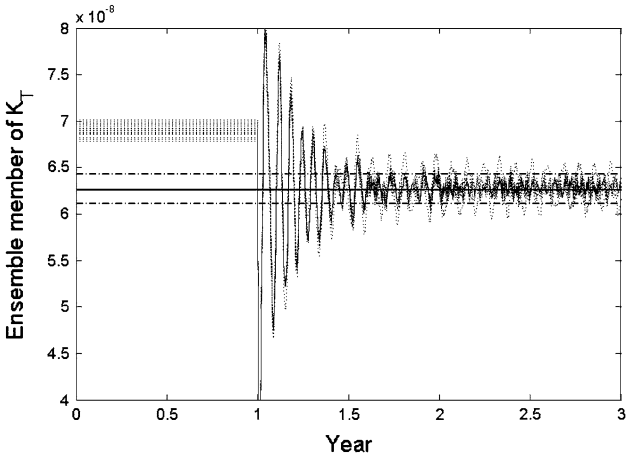

Fig. 2 Time series of the ensemble members of K_T for SPE scheme. The *dotted lines* represent the 20 ensemble members of K_T, the *black line* is the global mean of "truth" K_T and the *dot-dashed lines* indicate the *upper* (K_T at poles) and *lower* (K_T at equator) bounds of K_T. Note that parameter estimation is activated after 1 year's state estimation only (SEO)

In GPO, the value of σ_l in Eq. (6) is geographically dependent (we use the time average of sensitivities to estimate).The inflation factor α_0 is set to 1.0. During parameter optimization, the impact radius of observations of SST is assumed to be the same as state estimation. GPO optimizes K_T for each ocean grid using surrounding observations of SST. The initial K_T for each grid is set to the same biased value as in SEO. In order to avoid introducing large parameter gradient between the no-observation area and the ambient places, a simple linear interpolation of K_T is performed in the no-observation area. For each analysis step, after all K_T in other model grids being updated with observations of SST, each K_T that falls in this area is replaced by the linear interpolated value of the nearest four grids outside this place.

Figure 1 shows the truth (the thin solid line), the initial biased value (the dotted-dashed line) and the global mean (the thick solid line) of the truth of K_T, the time-averaged SPE-estimated (the dotted line) and the time-latitude averaged GPO-optimized (the dashed line) K_T. SPE improves the initial biased value significantly and approaches the global mean of the truth. Because the initial biased K_T is much larger than the maximal value (locates at poles) of truth K_T, SPE can drag the biased K_T around the global mean, and therefore improve the quality of SST in the mid latitudes. For GPO, it exactly tracks the truth value in the mid latitudes. For high latitudes, especially in Southern Hemisphere, GPO-optimized K_T is a little deviated from the "truth" which is caused by insufficient observation constraint there. Note that due to the linear variation of K_T from the poles to the equator, the linear interpolation can perfectly approach the "truth" value in the no-observation area. In the real world and a CGCM, the same smoothing scheme may not be able to attain such excellent result. Even so, we believe that the smoothed parameter will be better than the non-smoothed one and SPE-generated parameter, because the parameter values used to smooth the non-adjusted one are optimized by the local observations.

Figure 2 shows the time series of ensemble members (dotted lines) of SPE-estimated K_T, the global mean of "truth" values (the black line) and the upper (K_T at poles) and lower (K_T at equator) bounds (dot-dashed lines) of K_T. During the first half year of parameter estimation, the ensemble of K_T oscillates dramatically around the global mean, representing the spin-up period of parameter estimation. Afterwards, the ensembles reach a quasi-stationary state where they oscillate between the upper and lower bounds. Note that due to the lack of dynamic support for parameter, an over small α_0 in Eq. (6) can cause the parameter ensemble to lose its spread, i.e. filter divergence.

Figure 3 shows the spatial distribution of root mean square error (RMSE) of SST for CTL (panel a), SEO (panel b), SPE (panel d) and GPO (panel c). For better comparison, results of SEO, SPE and GPO in the data void region (bounded by the black line in panels b, c, d) are zoomed in as Fig. 3e (SEO), Fig. 3f (SPE) and Fig. 3g (GPO). Compared with CTL, SSTs are significantly improved by SEO and SPE. For SEO, due to the biased K_T which is far away from the "truth" values, the error of SST decreases from the equator towards both poles. Without observation constraint, the error of SST for SEO (Fig. 3e) is comparable to CTL. For SPE, the minimum error of SST locates at the

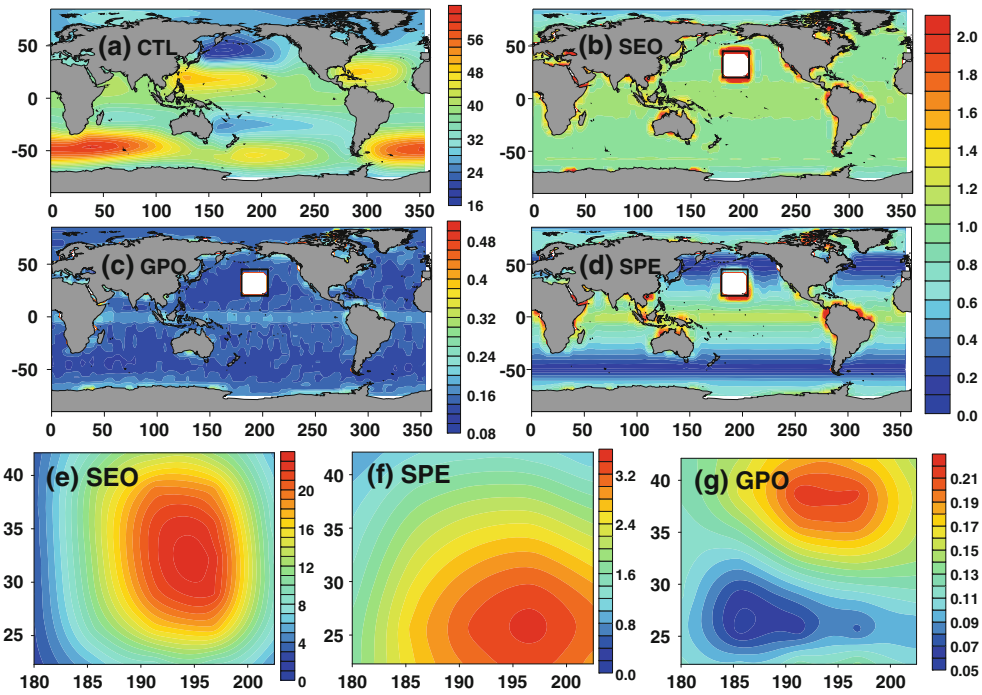

Fig. 3 The spatial distributions of the root mean square error (RMSE) of SST for control run (CTL, **a**), SEO (**b**, **e**), SPE (**d**, **f**) and GPO (**c**, **g**). **b**, **c**, **d** show the results in observed areas while **e**, **f**, **g** give the error distributions in no-observation areas (the *rectangle* area bounded by the *black line* in **b**, **c**, **d**). Note that **b** and **d** use the same *shade scale*

mid latitudes in both Hemispheres where the parameter is close to the truth. SPE applies the estimated K_T to all places including no-observation areas, which leads a systematic improvement of SST of SEO. However, without state estimation in the data void region, SPE can only partially reduce the error of SST (check with Fig. 3e, f). For GPO, it further reduces the error of SST for SPE in all places. Note, due to the fact that K_T is the sole error source of the assimilation model, the latitude-dependence of K_T in the "truth" model and the single value of K_T in SEO and SPE lead the zonal-distributed error of SST.

Figure 4 shows the time series of the RMSEs of the atmospheric streamfunction (panel a), the oceanic streamfunction (panel b), SST (panel c) and LST (panel d) for SEO (the blue line), SPE (the red line) and GPO (the green line) respectively. The small panel in panel b is the zoomed in version of the time series for the 5th year. Due to the coupling effects, improvements of SST for SPE and GPO also somewhat refine the atmospheric streamfunction and the oceanic streamfunction. Compared with SEO, because of the weak coupling between the land and other components, the improvements of LST for SPE and GPO are not as significant as those of the atmosphere and the ocean.

Figure 5 shows the spatial distributions of RMSEs of the atmospheric streamfunction (panels b, d, f) and the oceanic streamfunction (panels a, c, e) for SEO (panels a, b), SPE (panels c, d) and GPO (panels e, f). For SPE, the improvement of K_T in the data-void region refines fluxes from the ocean to the atmosphere, which further reduces the error of the atmospheric streamfunction (Fig. 5d). As such, the oceanic streamfunction is also improved (Fig. 5c). We found that the oscillation of K_T around the global mean can introduce noises into the atmospheric streamfunction in the mid and high latitudes (Fig. 5b), which further perturbs the oceanic streamfunction there (Fig. 5f). For GPO, due to the better SST caused by the optimized geographic dependent K_T, it further significantly ameliorates the atmospheric streamfunction and the oceanic streamfunction for SPE.

Figure 6 shows the time series of the RMSEs of SPE-estimated K_T (the dotted line) and GPO-optimized K_T (the dashed line). After 1 year's SEO spin-up period, there is another half year spin-up period of SPE while no spin-up period existing in GPO. Furthermore, the RMSE of GPO-optimized K_T is much smaller than that of SPE-estimated K_T. It's easy to infer that the minimum RMSE indicates that SPE estimates a global mean of "truth" for K_T.

Table 3 gives the total RMSEs of the atmospheric streamfunction (column 2), the oceanic streamfunction (column 3), SST (column 4) and LST (column 5) for CTL (row 2), SEO (row 3), SPE (row 4) and GPO (row 5) respectively. With state estimation, SEO, SPE and GPO dramatically reduce the error of all model states. Through parameter estimation, SPE and GPO further greatly refine the SST. Coupling effects lead the consistent improvement of other three variables. Due to the weak coupling between the land component and other ones, improvement of LST is not so significant. Compared with SPE, GPO reduces the RMSEs of the atmospheric streamfunction, the oceanic streamfunction, SST and LST by 14, 27, 81 and 0.5 %. On average, errors of model states are reduced by 31 %.

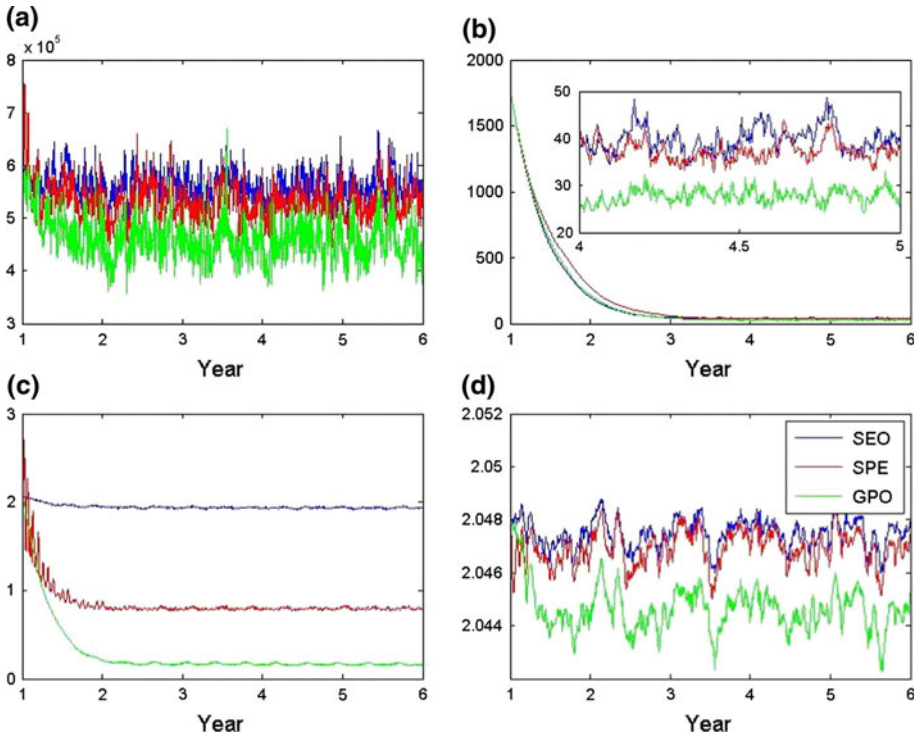

Fig. 4 Time series of the RMSEs of the atmospheric streamfunction (**a**), the oceanic streamfunction (**b**), SST (**c**) and LST (**d**) for SEO (*blue line*), SPE (*red line*) and GPO (*green line*). Note that first year's results are not shown here because of the same RMSEs for these three schemes

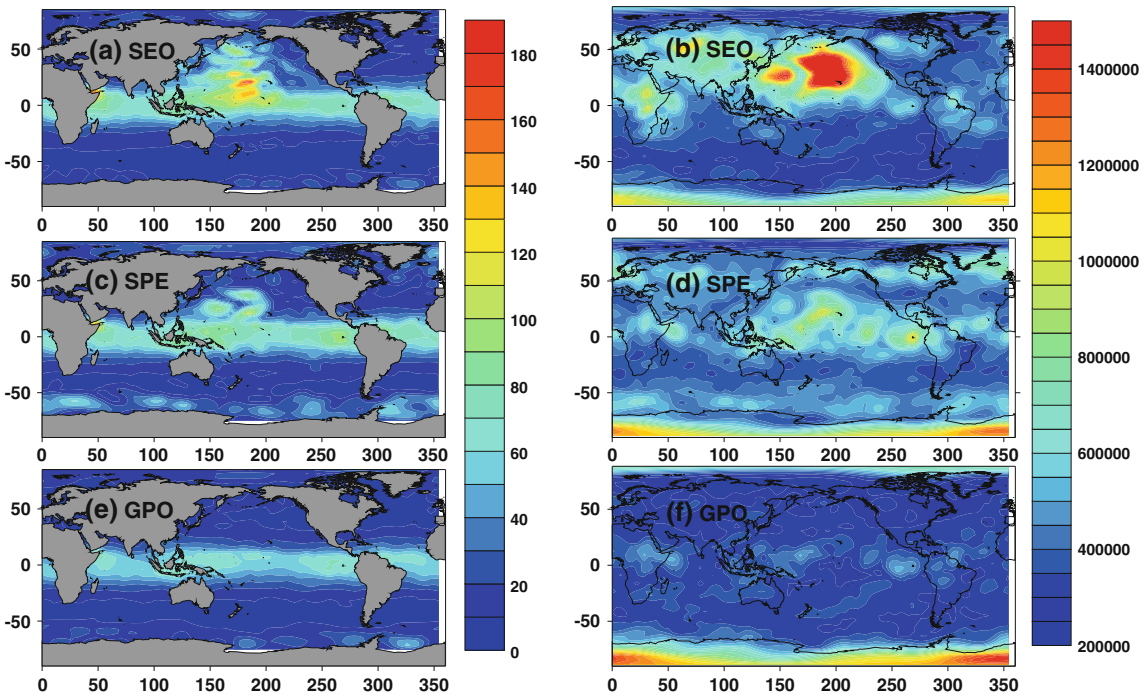

Fig. 5 The spatial distributions of the RMSEs of the oceanic streamfunction (**a**, **c**, **e**) and the atmospheric streamfunction (**b**, **d**, **f**) for SEO (**a**, **b**), SPE (**c**, **d**) and GPO (**e**, **f**). Note that **a**, **c**, **e** use the same *shade scale* while **b**, **d**, **f** use the same *shade scale*

Figure 7 shows the spatial distribution of the time-averaged GPO-optimized K_T. It is dominated by a zonal distribution and increases linearly from the equator towards both poles, both of which are consistent with the "truth" structure of K_T.

4 Evaluation of "climate" prediction skill

In order to evaluate the impact of observation-estimated parameter on model predictions, 20 forecast initial conditions are selected every 5 years apart from the SEO, SPE

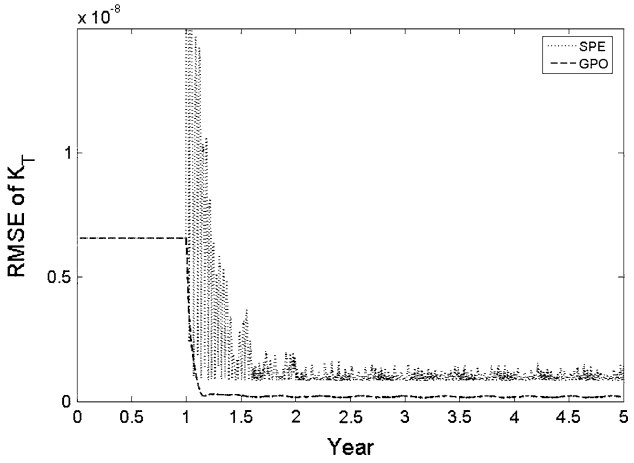

Fig. 6 Time series of the RMSEs of K_T for SPE (the *dotted line*) and GPO (the *dashed line*). Note that because parameter estimation is activated after 1 year's SEO, the RMSEs of K_T during the first year are the same for two schemes

Table 3 Total RMSEs of atmospheric streamfunction-ψ, oceanic streamfunction-φ, sea surface temperature (T_o) and land surface temperature (T_l) for all experiments

	ψ (m^2 s^{-1})	φ (m^2 s^{-1})	T_o (K)	T_l(K)
CTL	42858182.3	17685.89	37.93	2.89
SEO	561773.0	40.27	1.93	2.05
SPE	527109.9	37.77	0.79	2.05
GPO	453397.5	27.62	0.15	2.04

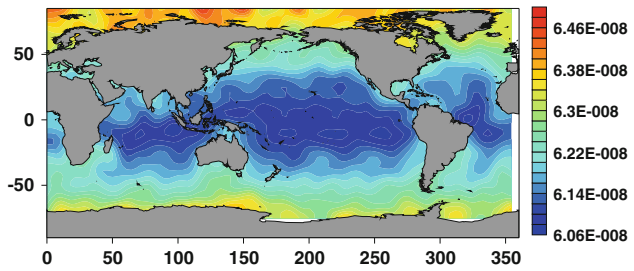

Fig. 7 The spatial distribution of GPO-optimized K_T

and GPO analysis fields in the period of 5–100 years. Then 20 initial fields are forwarded up to 10 years for these three assimilation schemes. Here, the global anomaly correlation coefficient (ACC) of the forecasted ensemble mean is used to evaluate the global pattern correlation with the "truth"; the global RMSE of the forecasted ensemble mean is used to evaluate the global absolute error with respect to the "truth". However in the real world with instrumental data, the error of the innovation of forecasts to observations may be a more appropriate quantity to evaluate forecast skills of different data assimilation schemes (see e.g. Fukumori et al. 1999).

We first examine the "climate" prediction skill. The discrepancy between SEO-used and SPE-estimated K_T and the "truth" K_T causes the initial ACCs of SST very low (about 0.2–0.3, the solid line and the dotted line in Fig. 8a). After 2 month's lead time, ACCs of both SEO and SPE drop to around 0. By contrast, the GPO-optimized K_T can retrieve the major spatial structure of the "truth" K_T, which effectively enhances the initial ACC (about 0.8, the dashed line in Fig. 8a) of SST. Because K_T dominates the SST equation, erroneous K_T in SEO, which is far away from all the "truth" values of K_T, makes the RMSE of SST (see the solid line in Fig. 8b) increase rapidly and dramatically. SPE-estimated K_T approaches the global mean of the "truth" values, which greatly reduces the RMSE of SST (see the dotted line in Fig. 8b). With the GPO-optimized K_T, RMSE of SST is further reduced significantly. Comparison between SPE and GPO for the first 2 months' "climate" forecast lead time shows that the averaged ACC of SST is increased by 379 % from 0.14 to 0.67 and the averaged RMSE is reduced by 83 % from 1.34 to 0.23 K.

Then we evaluate the "weather" forecast skill. Figure 8c and d show the variations of ACC and RMSE with 14 days' forecast lead time of the forecasted ensemble means of the atmospheric streamfunction for SEO (the solid line), SPE (the dotted line) and GPO (the dashed line). With coupling effect between the ocean and the atmosphere components, GPO-optimized K_T greatly improves SST and thus refines the atmospheric streamfunction, which leads to the highest ACC and the smallest RMSE. For SEO and SPE, the incorrect structure of K_T disturbs the atmosphere and reduces the "weather" forecast skill. It's also very interesting that SPE loses its superiority relative to SEO after about 5 days' forecast lead time, which may be caused by many uncertain reasons. Comparison between SPE and GPO for the first 14 days' "weather" forecast lead time shows that the averaged ACC of the atmospheric streamfunction is increased by 4 % from 0.79 to 0.82 and the averaged RMSE is decreased by 5 % from 4,005,831 to 3,808,744 m^2 s^{-1}. If we roughly combine the RMSE and ACC results of the "climate" prediction and the "weather" forecast for SPE and GPO, the forecast skill of SPE is nearly doubled by GPO.

5 Summary and Discussions

A twin experiment framework with an intermediate coupled model is designed to investigate the impact of the geographic dependence of observing system on parameter estimation. In this framework, some model parameter (physics) in the "truth" model that is used to produce "observations" is allowed to vary geographically so as to simulate the geographic dependence of representation of

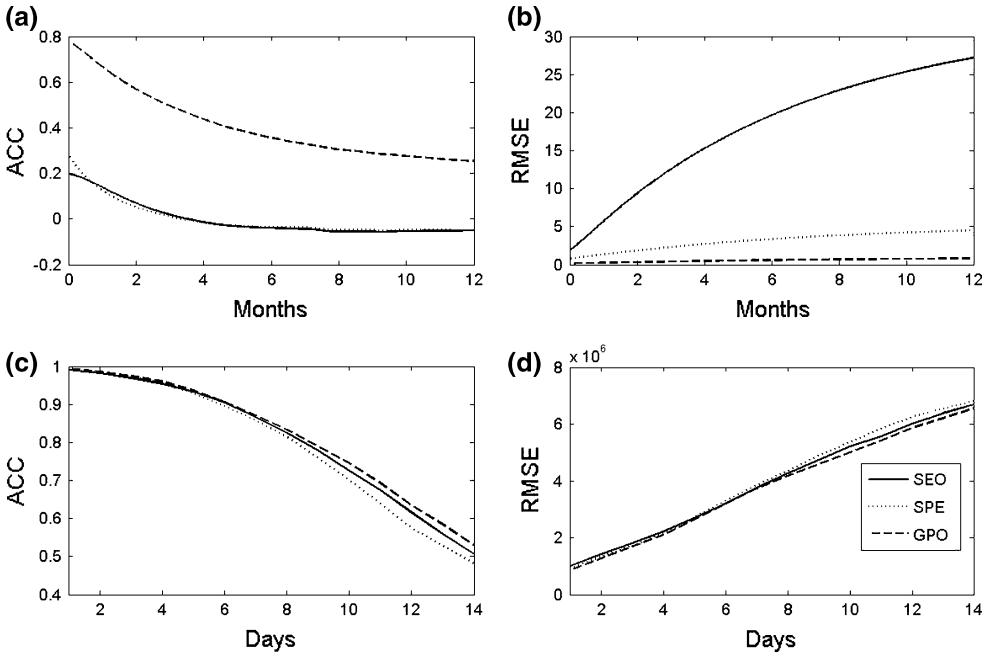

Fig. 8 Variations of anomaly correlation coefficient (ACC) (**a**, **c**) and RMSE (**b**, **d**) with the forecast lead time of the forecasted ensemble means of SST (**a**, **b**) and the atmospheric streamfunction (**c**, **d**) and for SEO (*the solid line*), SPE (*the dotted line*) and GPO (*the dashed line*)

observational information, while the corresponding parameter in the assimilation model takes the first guess with a biased single value. Furthermore, observations in some area are removed to study the impact of geographic dependent observational coverage.

"Observations" are assimilated into the assimilation model to implement SEO, single-valued parameter estimation (SPE) and GPO. Results show that the SPE-estimated parameter approaches the global mean of the "truth" values. Localization of the parameter makes GPO exactly retrieve the "truth" structure of the parameter, which systematically reduces the errors of model state in observed places. Through coupling effects, other model variables can be consistently improved by the parameter estimation. It's worth mentioning that an appropriate smoothing can effectively enhance the signal of the parameter in the no-observation area and further improves the quality of state estimates. Forecast experiments show that GPO-optimized parameter can greatly improve the model predictability.

Although promises are shown with the simple model, there are considerable challenges remained when the GPO scheme is applied to the real climate observing system with a CGCM. First, besides the uncertainty induced by model parameters, many other model bias sources exist. How multiple model biases influence the quality of parameter estimation shall be examined. Second, the observing system in the real world is much more complicate than the simple case in this study. The impact of a more realistic observing system shall be further investigated. Third, a simple linear interpolation is employed here in parameter estimation for the observation-void places; an advanced interpolation scheme (Yang et al. 2009) may have impact on the results and needs be examined. Last, the inflation in GPO is determined by trial-and-error tuning, and an adaptive scheme (Anderson 2008; Miyoshi 2011) may be helpful for CGCM applications.

Acknowledgments The authors thank three anonymous reviewers for their thorough comments that are very helpful for improving the manuscript. This research is sponsored by NSF, 2012CB955201 and NSFC, 41030854.

References

Aksoy A, Zhang F, Nielsen-Gammon JW (2006a) Ensemble-based simultaneous state and parameter estimation with MM5. Geophys Res Lett 33:L12801. doi:10.1029/2006GL026186

Aksoy A, Zhang F, Nielsen-Gammon JW (2006b) Ensemble-based simultaneous state and parameter estimation in a two-dimensional sea-breeze model. Mon Weather Rev 134:2951–2970

Anderson JL (2001) An ensemble adjustment Kalman filter for data assimilation. Mon Weather Rev 129:2884–2903

Anderson JL (2003) A local least squares framework for ensemble filtering. Mon Weather Rev 131:634–642

Anderson JL (2008) Spatially and temporally varying adaptive covariance inflation for ensemble filters. Tellus 61A:72–83

Annan JD, Hargreaves JC (2004) Efficient parameter estimation for a highly chaotic system. Tellus 56A:520–526

Asselin R (1972) Frequency filter for time integrations. Mon Weather Rev 100:487–490

Banks HT (1992a) Control and estimation in distributed parameter systems. In: Banks HT (ed) Frontiers in applied mathematics, vol 11. SIAM, Philadelphia, p 227

Banks HT (1992b) Computational issues in parameter estimation and feedback control problems for partial differential equation systems. Physica D 60:226–238

Borkar VS, Mundra SM (1999) Bayesian parameter estimation and adaptive control of markov processes with time-averaged cost. Appl Mathemat 25(4):339–358

Fukumori I, Raghunath R, Fu L, Chao Y (1999) Assimilation of TOPEX/POSEIDON data into a global ocean circulation model: how good are the results? J Geophys Res 104:25,647–25665

Hamill TM, Whitaker JS, Snyder C (2001) Distance-dependent filtering of background error covariance estimates in an ensemble Kalman filter. Mon Weather Rev 129:2776–2790

Hansen J, Penland C (2007) On stochastic parameter estimation using data assimilation. Physica D 230:88–98

Jazwinski AH (1970) Stochastic processes and filtering theory. Academic Press, New York, p 376

Kalman R (1960) A new approach to linear filtering and prediction problems. Trans ASME Ser D J Basic Eng 82:35–45

Kalman R, Bucy R (1961) New results in linear filtering and prediction theory. Trans ASME Ser D J Basic Eng 83:95–109

Kang JS (2009) Carbon cycle data assimilation using a coupled atmosphere-vegetation model and the local ensemble transform Kalman filter. Ph.D Dissertation, University of Maryland, pp. 164

Kang JS, Kalnay E, Liu J, Fung I, Miyoshi T, Ide K (2011) "Variable localization" in an ensemble Kalman filter: Application to the carbon cycle data assimilation. J Geophys Res 116:D09110. doi: 10.1029/2010JD014673

Kondrashov D, Sun C, Ghil M (2008) Data assimilation for a coupled ocean-atmosphere model, part II: parameter estimation. Mon Weather Rev 136:5062–5076

Kulhavy R (1993) Implementation of Bayesian parameter estimation in adaptive control and signal processing. J Royal Stat Soc Ser D (The Statistician) 42(4):471–482

Liu Z (1993) Interannual positive feedbacks in a simple extratropical air-sea coupling system. J Atmos Sci 50:3022–3028

Miyoshi Takemasa (2011) The Gaussian approach to adaptive covariance inflation and its implementation with the local ensemble transform Kalman filter. Mon Weather Rev 139:1519–1535

Philander G, Yamagata T, Pacanowski RC (1984) Unstable air-sea interaction in the tropics. J Atmos Sci 41:604–613

Robert A (1969) The integration of a spectral model of the atmosphere by the implicit method. Proceeding of WMO/IUGG symposium on NWP. Japan Meteorological Society, Tokyo, Japan, 19–24

Tao G (2003) Adaptive control design and analysis. Wiley, Hoboken, p 640

Tong M, Xue M (2008a) Simultaneous estimation of microphysical parameters and atmospheric state with simulated Radar data and ensemble square root Kalman filter. Part I: sensitivity analysis and parameter identifiability. Mon Weather Rev 136:1630–1648

Tong M, Xue M (2008b) Simultaneous estimation of microphysical parameters and atmospheric state with simulated Radar data and ensemble square root Kalman filter. Part II: parameter estimation experiments. Mon Weather Rev 136:1649–1668

Wu X, Zhang S, Liu Z, Rosati A, Delworth T, Liu Y (2012) Impact of geographic dependent parameter optimization on climate estimation and prediction: simulation with an intermediate coupled model. Mon Weather Rev (under revision)

Yang Shu-Chih, Kalnay E, Hunt B, Bowler NE (2009) Weight interpolation for efficient data assimilation with the local ensemble transform Kalman Filter. Quart J Royal Meteor Soc 135:251–262

Zhang S (2011a) Impact of observation-optimized model parameters on decadal predictions: simulation with a simple pycnocline prediction model. Geophys Res Lett 38:L02702. doi: 10.1029/2010GL046133

Zhang S (2011b) A study of impacts of coupled model initial shocks and state-parameter optimization on climate prediction using a simple pycnocline prediction model. J Clim 24:6210–6226

Zhang S, Anderson JL (2003) Impact of spatially and temporally varying estimates of error covariance on assimilation in a simple atmospheric model. Tellus 55A:126–147

Zhang S, Anderson JL, Rosati A, Harrison MJ, Khare SP, Wittenberg A (2004) Multiple time level adjustment for data assimilation. Tellus 56A:2–15

Zhang S, Harrison MJ, Rosati A, Wittenberg AT (2007) System design and evaluation of coupled ensemble data assimilation for global oceanic climate studies. Mon Weather Rev 135:3541–3564

Zhang S, Liu Z, Rosati A, Delworth T (2011) A study of enhancive parameter correction with coupled data assimilation for climate estimation and prediction using a simple coupled model. Tellus 63A:10963. doi:10.3402/tellusa.v63i0.10963